Available online at www.sciencedirect.com

ScienceDirect

Geochimica et Cosmochimica Acta 128 (2014) 128–143

Geochimica et Cosmochimica Acta

www.elsevier.com/locate/gca

Iron isotopes in the Seine River (France): Natural versus anthropogenic sources

Jiu-Bin Chen [a,b,*], Vincent Busigny [b], Jérôme Gaillardet [b,c], Pascale Louvat [b], Yi-Na Wang [a]

[a] State Key Laboratory of Environmental Geochemistry (SKLEG), Institute of Geochemistry, Chinese Academy of Science, Guiyang 550002, China

[b] Institut de Physique du Globe de Paris, Sorbonne Paris Cité, Univ. Paris Diderot, UMR 7154 CNRS, 1 rue Jussieu, 75238 Paris, France

[c] Institut Universitaire de France, France

Received 3 October 2013; accepted in revised form 12 December 2013; available online 21 December 2013

Abstract

The determination of fluxes and isotope compositions of Fe transported from continents to the ocean is essential for understanding global surface Fe cycle and its effect on oceanic biological productivity. Contrasting to non-polluted rivers, Fe isotope composition in rivers strongly affected by human activities is poorly constrained. In this contribution, we present the first Fe isotope data in suspended particulate matter (SPM) and dissolved load of the human-impacted Seine River (France). Iron concentrations and isotope compositions, together with major and trace element concentrations, were measured for two sample sets: (1) a geographic transect along the river from headwater to estuary, and (2) a temporal series of samples collected in Paris from 2004 to 2007. In the Seine River, Fe is mostly carried by SPM (average 99% of the total Fe) rather than dissolved load. The high Fe enrichment factor (1.40, relative to natural fluvial pre-historical and headwater sediments) and strong correlation between SPM Fe and Zn concentrations ($r^2 = 0.70$, $n = 30$) demonstrate a strong anthropogenic Fe input. The Fe isotope compositions in SPM show a very small range (δ^{56}Fe from −0.05‰ to 0.09‰) in spite of the large variations of Fe concentrations (from 1.78 to 4.17 wt.%) and are comparable to anthropogenic samples, suggesting that anthropogenic sources have similar Fe isotope composition to that of the natural background. In contrast, larger variations of Fe isotope compositions observed in the dissolved load (from −0.60‰ to 0.06‰) than that of SPM may provide a more promising means for tracing anthropogenic contributions to natural river systems. The δ^{56}Fe and δ^{66}Zn values of the dissolved loads are positively correlated ($r^2 = 0.62$, $n = 8$), indicating a mixing between anthropogenic and natural end-members, enriched in light and heavy Fe isotopes respectively. Correlation between dissolved δ^{56}Fe and DOC/Fe ratio (i.e. dissolved organic carbon/dissolved Fe concentrations) suggests that dissolved Fe of natural origin is mainly associated with organic colloids. The Fe compounds with low DOC/Fe ratio and δ^{56}Fe values may correspond to anthropogenically-derived Fe-oxyhydroxide or sulfide colloids. Our study clearly demonstrates that polluted rivers transport an anthropogenic surplus flux of Fe that can be traced by coupling Fe and Zn isotopes. This surplus flux will fertilize the ocean and increase the primary productivity of phytoplankton, and thus may ultimately impact the global carbon cycle.

1. INTRODUCTION

Iron is an essential element for biogeochemical and physiological functioning of terrestrial and oceanic organisms, and in particular of phytoplankton, which is responsible for the primary productivity in the world ocean

* Corresponding author at: State Key Laboratory of Environmental Geochemistry (SKLEG), Institute of Geochemistry, Chinese Academy of Science, Guiyang 550002, China. Tel.: +86 851 5892669.

E-mail address: chenjiubin@vip.gyig.ac.cn (J.-B. Chen).

0016-7037/$ - see front matter © 2013 Elsevier Ltd. All rights reserved.
http://dx.doi.org/10.1016/j.gca.2013.12.017

(Morel and Price, 2003). Changes in the supply of Fe to the ocean may lead to climate change by affecting biological productivity and alter rates of carbon sequestration (Martin, 1990; Anbar and Knoll, 2002; Blain et al., 2007). It is thus crucial to precisely determine the variations of Fe fluxes to the ocean in modern environment and assess its effect on primary productivity. The fluxes of Fe delivered to the ocean can potentially be traced using Fe isotopes and derive mainly from hydrothermal systems, atmospheric dust, and continental weathering products transferred by rivers (Beard et al., 2003; Fantle and DePaolo, 2004). The flux of diagenetic Fe released from marine sediments is probably also significant (Severmann et al., 2010). Indeed, Fe(II) produced from Fe(III) reduction during burial processes in marine sediments diffuses back to the water column either as dissolved Fe(II) or organic colloids. This benthic Fe flux is usually enriched in light isotopes relative to the mean Fe isotopic composition of sediments (Severmann et al., 2006; Staubwasser et al., 2006; Homoky et al., 2009), but locally, enrichment in heavy Fe isotopes of porewaters can be produced, for instance by precipitation of Fe sulfides that incorporate preferentially light isotopes (Butler et al., 2005; Roy et al., 2012).

The Fe isotope budget of particulate and dissolved loads transported by rivers to the ocean is still in its infancy and is poorly constrained (Fantle and DePaolo, 2004; Bergquist and Boyle, 2006; Ingri et al., 2006; Escoube et al., 2009; Song et al., 2011). In their pioneer work, Fantle and DePaolo (2004) analyzed several rivers from Western United States and Canada, spanning a range of Fe concentration and weathering regimes. They observed that riverine particles generally had δ^{56}Fe values near 0.07‰, similar to igneous rocks and the continental crust (Poitrasson, 2006). In contrast, dilute streams had negative δ^{56}Fe values down to ~−1‰, suggesting that dissolved riverine Fe was characterized by light isotopes. Iron isotope studies of the Amazon River reported overall large δ^{56}Fe variation (Bergquist and Boyle, 2006; dos Santos Pinheiro et al., 2013). Identical δ^{56}Fe values of about -0.2 ± 0.1‰ was found by Bergquist and Boyle (2006) for both dissolved and suspended loads of two main channel samples, while relatively high δ^{56}Fe values were found for the dissolved load (+0.30‰) of an organic-rich tributary compared to the associated suspended load (−0.90‰). Overall, the bulk δ^{56}Fe value (−0.30‰) of this organic-rich river was similar to other tributaries (Bergquist and Boyle, 2006). However, dos Santos Pinheiro et al. (2013) reported δ^{56}Fe values of about 0.07‰ for suspended particles in the Amazon River and its major tributaries, with lower value (−0.20‰) only for the Negro river SPM. Iron isotope composition in the suspended fraction of a boreal river suggested that Fe was carried by two main phases as Fe-oxyhydroxides and Fe bound to organic carbon, being respectively enriched in heavy and light isotopes (Ingri et al., 2006). This interpretation was recently challenged by a detailed study of boreal and temperate organic-rich waters, treated by cascade filtration and ultrafiltration, showing that Fe-poor, C-rich colloids were enriched in heavy Fe isotopes relative to Fe-rich, C-poor colloids (Ilina et al., 2013).

Studies on soil formation and continental weathering are also essential for determining the range of δ^{56}Fe values of the Fe products released and transferred to the ocean through rivers (Brantley et al., 2001, 2004; Emmanuel et al., 2005; Thompson et al., 2007; Guelke et al., 2010; Yesavage et al., 2012). By coupling experiments and natural observations on soil, previous studies showed that the fraction of exchangeable Fe was generally enriched in light isotopes relative to Fe-oxyhydroxides or silicate-rich substrates (Brantley et al., 2001, 2004; Guelke et al., 2010). This light isotope signature of the exchangeable Fe in soils was likely the result of complex interplays among ferric iron reduction by micro-organisms (Beard and Johnson, 1999; Crosby et al., 2005; Johnson and Beard, 2005), adsorption of isotopically heavy ferrous iron on soil minerals (Icopini et al., 2004; Dideriksen et al., 2008), and formation of Fe-rich organic ligands (Brantley et al., 2004; Ingri et al., 2006).

To date, all previous studies of Fe isotope systematics focused only on non-polluted rivers, while none of them attempted to characterize the impact of human activities. In the present contribution, Fe isotope compositions were determined in both suspended particulate matters (SPM, $n = 31$) and dissolved load ($n = 9$) of samples from the Seine River (France) in order to assess the potential of Fe isotope for tracing anthropic contamination. Two series of samples were analyzed: (1) a geographic transect along the Seine River from headwater to estuary, in order to assess variations above the natural background and thus identify contamination by human activity and (2) a monthly sampling in Paris between 2004 and 2007, monitoring temporal variations associated with low-and high water stages. Additionally, several samples from potential anthropogenic sources and headland bedrocks were also analyzed. This study builds on our previous works on Zn isotopes for both dissolved and suspended loads, which showed a large impact of human activities on Zn geochemical cycling (Chen et al., 2008, 2009a). Since the particulate phase is the overwhelming carrier of riverine Fe transported into the ocean, we focus mainly on Fe isotopic composition of the Seine SPM. In this paper, Fe isotope composition of SPM is coupled with major and trace element concentrations, organic carbon content, and Zn isotope composition to better determine the natural *vs.* anthropogenic contributions of Fe to the Seine River. Results show that particulate Fe derived from anthropogenic sources is isotopically undistinguishable from natural contributions, while the dissolved Fe displays relatively large variation of δ^{56}Fe values, demonstrating stronger potential of Fe isotopes in the dissolved load for tracing Fe sources and chemical reactions in river systems.

2. SAMPLES

The Seine River (France) is one of the most human-impacted rivers in Europe, with high concentrations of metals (Zn, Cu, Pb, Ni, Cd, etc.) in both dissolved and suspended loads compared to large rivers worldwide (Gaillardet et al., 2005; Meybeck et al., 2007; Thévenot et al., 2007; Chen et al., 2008, 2009a). The Seine basin (Fig. 1) displays two

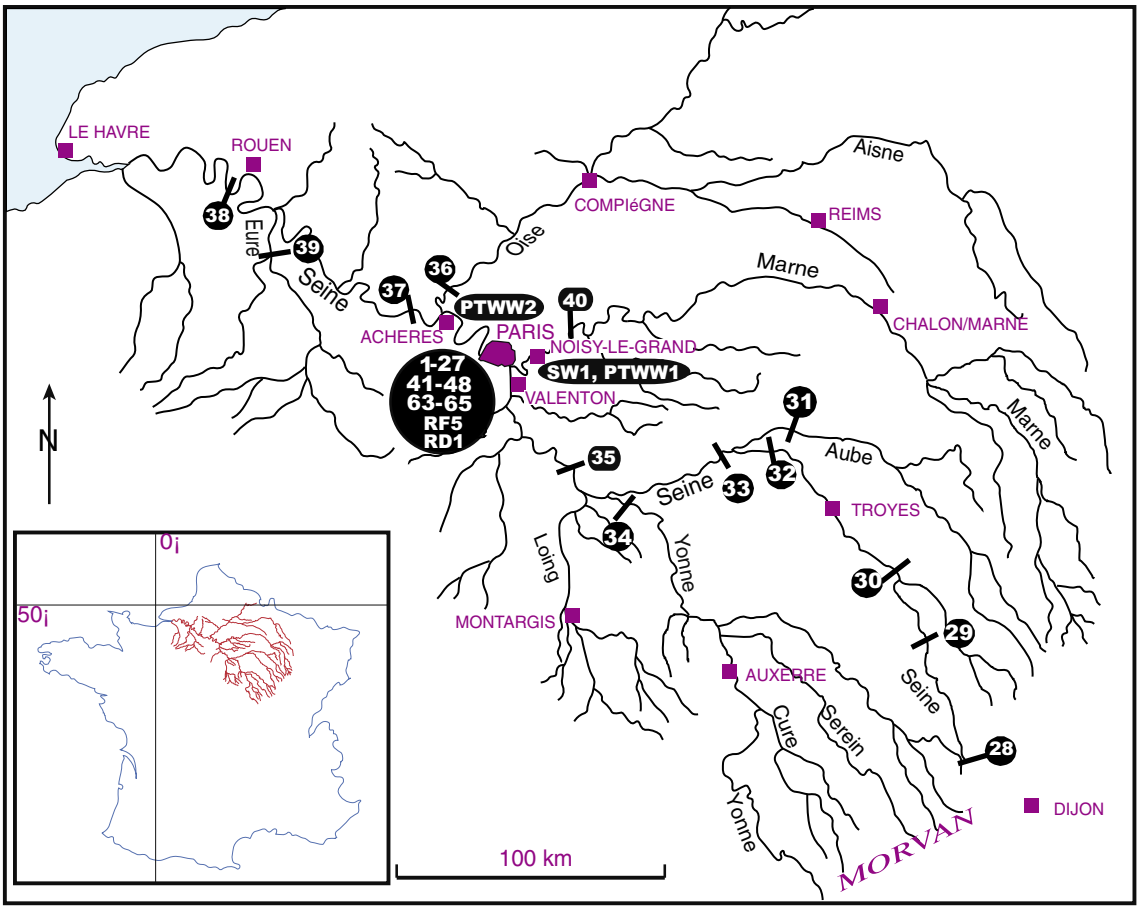

Fig. 1. Map of the Seine basin and sampling locations. Sampling description is detailed in the main text (Section 2).

important characteristics: a relatively simple carbonate-dominated lithology and an increasing anthropogenic impact from the headland towards the estuary. The whole basin drains a surface area of 79,000 km^2 and is mostly covered by carbonate-clay rocks (Jurassic limestones, Cretaceous marls and chalks, and Tertiary argillaceous limestones and marls), except for the southern part (Morvan area, 2000 km^2) where Hercynian gneissic, granitic and rhyolitic rocks are found (Roy et al., 1999; Chen et al., 2009a). The Seine River basin is intensely cultivated. Industrial activities are concentrated mostly in Paris conurbation and downstream from Paris. Only the headwater streams of the Yonne, the Seine and the Aube rivers drain relatively pristine forested areas. About 16 million people live in the Seine River basin (average 215 people per km^2), with a strong gradient of population density: from 10 persons per km^2 in the headwater regions to about 5000 persons per km^2 in Paris area (Chetelat and Gaillardet, 2005; Meybeck et al., 2007).

The long-term mean water discharge of the Seine River is about 260 m^3/s at Paris and average suspended sediment concentration is estimated to be 44 mg/L, which is low in comparison to the world average of ~100 mg/L (Roy et al., 1999; Gaillardet et al., 2005). In summer, the concentration of suspended sediments decreases, but can reach >150 mg/L during floods. The main source of SPM in the Seine River is from the sedimentary terrains (loess and fluvial deposits) of Jurassic and Tertiary age that cover the Seine basin (Roy et al., 1999; Chen et al., 2009a). The geochemistry of SPM shows high degrees of chemical depletion for the most soluble elements (i.e. Na, K and Mg) and suggests that they are derived from materials that have experienced one or more cycles of weathering and deposition (Roy et al., 1999; Chen et al., 2009a). The major element chemical composition of the Seine SPM is thus typical of platform shaly-carbonates, while trace metals such as Zn, Cu, Pb have relatively high concentrations compared to the natural background, due to anthropogenic inputs (Roy et al., 1999; Thévenot et al., 2007; Chen et al., 2008, 2009a; Priadi et al., 2012).

Two series of samples were collected in the Seine basin between May 2004 and March 2007 for Fe isotope measurement (Fig. 1). The time series was sampled monthly or bimonthly near the IPGP Campus in Paris at different hydrological stages (water discharge ranging from 100 to 1100 m^3/s). The second set of samples was collected along a geographical transect of the Seine River basin from the headwaters to the estuary, during the flood of February 22nd, 2006, and includes samples from tributaries (Aube, Yonne, Loing, Marne, Oise, and Eure Rivers). In an attempt to identify natural and anthropogenic sources of Fe input to the Seine River, complementary samples were also

analyzed, including a limestone of Cretaceous Chalk formation (from Provins) and a granite (from Morvan region) supposed to be representative of the Seine basin headland, and urban anthropogenic samples consisting of a roof runoff (RF5), a roadway runoff (RD1), an untreated sewage water (SW1) and two plant-treated wastewaters (PTWW1 and 2) collected in Paris Conurbation (Fig. 1).

3. METHODS

All vials (en Teflon for Zn separation and en PP for water sampling) were conditioned with ultra-pure distilled HNO_3 and rinsed with MilliQ H_2O just before their use. River samples were collected with an acid-cleaned 2 L PP sampler, 1.5 m below the water surface (Chen et al., 2008, 2009a,b). Fifteen liters of water were collected in a clean plastic container in order to obtain the required mass (>50 mg) of SPM for chemical and Fe and Zn (Chen et al., 2009a) isotopic analyses. Samples were immediately filtered with 0.2 μm membrane filters (polysulfone ether, diameter 142 mm). Three 60 ml bottles were filled with filtrated sample, one 60 ml bottle was kept non-acidified for anions determination by HPLC, while the others were acidified to pH 2 with ultra-pure HNO_3, for major (HPLC and ICP-AES) and trace (ICP-MS) element analysis. The particulate phases were isolated by collecting SPM both deposited on filters and settled at the bottom of the container. We ensured that the recovery of SPM were close to 100% by comparing the collected particulate mass to the quantity obtained from independently filtering waters (250 ml to 1 L) with a smaller filtration unit (47 mm filter diameter).

A set of SPM samples were analyzed for major and trace element concentrations at the Service d'Analyse des Roches et des Minéraux (SARM) in Nancy, France, while others were measured at IPGP. SPM samples were dried at 60 °C and crushed in an agate mortar. Approximately 30 mg of powdered SPM were dissolved in a mixture of concentrated ultra-pure HNO_3 and HF (0.5 ml 16 M HNO_3 and 0.5 ml distilled 27 M HF) for ~12 h at 120 °C. After evaporation at 90 °C, the residue was digested twice, with first 1 ml 16 M HNO_3 and then 0.6 ml 0.9 M H_3BO_3 mixed with 0.15 ml 16 M HNO_3. The final residue was dissolved in 2 ml distilled 6 M HCl for chemical purification and an aliquot dissolved in 2% HNO_3 for major and trace element concentration measurement by ICP-OES (Inductively Coupled Plasma–Optical Emission Spectrometry, Thermo Fischer ICap 6500) and ICP-MS (Inductively Coupled Plasma Mass Spectrometry, Agilent 7700X), respectively. Analytical quality of trace element measurement was controlled by internal standard addition (In and Re) and regular international geo-standard (i.e. SLRS4) measurements. The precision for concentrations of most trace elements was generally better than 5%. After carbonate removal by HCl digestion, the concentration of particulate organic carbon (POC) was measured by EA (Carlo-Erba NA-1500NC), when sufficient SPM was available (Chen et al., 2009a). First-order mineralogy of the Seine River SPM was investigated using X-ray Diffraction (XRD, UltraX 18HF Rigaku) and Scanning Electron Microprobe (SEM, ΣIGMA, GEMINI). Iron concentrations of filtrated water samples were measured either by ICP-OES or MC-ICP-MS (Multiple Collector ICP-MS, Neptune) after evaporation and purification (for Fe isotope analysis, see below) with a precision better than 8%. Dissolved organic carbon (DOC) was measured on TOC-V_{CSH} (Shimadzu) for dissolved load.

Iron in SPM samples was extracted by anion-exchange chromatography according to a new chemical procedure (Chen et al., 2009a) based on the method of Marechal et al. (1999) and is only summarized in the following part. Digested SPM samples (in 1 ml 6 M HCl) were loaded onto the column filled with 1.6 ml AG MP-1 resin. After rinsing the matrix with 10 ml 6 M HCl and eluting Cu with 20 ml 6 M HCl, Fe was collected in 10 ml 2 M HCl. The addition of 10 ml 0.5 M HNO_3 allowed for the collection of Zn. The final Fe fraction was evaporated and re-dissolved in 0.3 M HNO_3 for MC-ICP-MS measurement. The whole separation procedure led to Fe yields close to 100% for most samples, checked by comparison with Fe concentrations measured previously by ICP-MS. The total Fe procedural blank (SPM digestion and ion-exchange separation) was about 30 ng. This blank contribution had no significant influence on Fe isotopic measurements as the typical sample size was ~10 μg of Fe. In order to test the accuracy of this method, 4 SPM samples were also processed using anion-exchange chromatography (AG1-X8 resin), following the protocol developed by Dauphas et al. (2004). Both methods gave identical results (Table 1). The Fe isotopic composition of dissolved loads was measured in 9 samples (six transect samples and three samples in Paris) after evaporation and Fe purification similar to SPM.

Iron isotope analyses were performed on a Neptune (Thermo Scientific) MC-ICP-MS at the Laboratoire de Géochimie et Cosmochimie, IPGP. Iron isotopes were measured simultaneously at masses 54, 56, 57 and 58. The contributions of Cr and Ni on masses 54 and 58 were monitored and corrected for using ion intensities measured at masses 53 and 60, respectively. Iron isotopes were fully resolved from argide interferences (mainly $^{40}Ar^{14}N^+$, $^{40}Ar^{16}O^+$, $^{40}Ar^{16}OH^+$ and $^{40}Ar^{18}O^+$ interfering at m/z 54, 56, 57 and 58) using the high-resolution mode (Weyer and Schwieters, 2003; Dauphas and Rouxel, 2006). Sample solutions were nebulized and introduced into the plasma using the ESI Apex-HF desolvating apparatus. Iron isotopes were measured in 0.3 M HNO_3 at a concentration of ~0.6 ppm Fe that gave a signal intensity on the mass 56 between 10 and 15 volts. Instrumental mass discrimination was corrected for using the conventional sample-standard bracketing (SSB) approach (Belshaw et al., 2000; Beard et al., 2003; Rouxel et al., 2003; Albarède and Beard, 2004). The SSB method was shown to give results as accurate and precise as Cu-doping method for correction of instrumental mass bias during Fe isotope measurement (Schoenberg and von Blanckenburg, 2005; Dauphas et al., 2009). The $^{56}Fe/^{54}Fe$ and $^{57}Fe/^{54}Fe$ ratios were expressed in the usual δ notation in per mil (‰) as:

$$\delta^{56}Fe = \lfloor (^{56}Fe/^{54}Fe)_{sample}/(^{56}Fe/^{54}Fe)_{standard} - 1 \rfloor \times 1000 \quad (1)$$

Table 1
Iron isotope composition ($\delta^{56}Fe$) of 4 SPM samples measured after chromatography purification using AG MP-1 resin (this study) and AG1-X8 resin (method described in Dauphas et al., 2004).

SPM sample	S12	S14	RF1	PTWW2
AG MP-1	-0.05 ± 0.06	-0.07 ± 0.07	0.17 ± 0.07	0.16 ± 0.04
AG 1-X8	-0.06 ± 0.04	-0.01 ± 0.06	0.14 ± 0.05	0.13 ± 0.05

The analytical uncertainty on $\delta^{56}Fe$ values represents external error expressed as 2 standard deviations (2SD); see the text for samples description.

$$\delta^{57}Fe = \lfloor (^{57}Fe/^{54}Fe)_{sample}/(^{57}Fe/^{54}Fe)_{standard} - 1 \rfloor \times 1000 \quad (2)$$

where the standard is IRMM-014, a pure synthetic Fe metal from the Institute for Reference Materials and Measurements (Taylor et al., 1992). The accuracy and analytical precision were evaluated from the long-term analysis of three geo-standards (IF-G, a 3.8 Ga old Banded Iron Formation (BIF) from Isua, Greenland; BCR-2, a basalt from Columbia River, Portland, Oregon; AC-E, a granite from Ailsa Craig Island, SW Scotland). Mean $\delta^{56}Fe$ values of IF-G (102 analyses of 23 solutions), BCR-2 (59 analyses of 10 solutions) and AC-E (29 analyses of 5 solutions) were respectively $0.64 \pm 0.05‰$, $0.08 \pm 0.06‰$, and $0.34 \pm 0.05‰$ (2 Standard Deviation, 2SD), in good agreement with available data for these geo-standards (e.g. $0.64 \pm 0.05‰$, $0.09 \pm 0.05‰$ and $0.32 \pm 0.05‰$, Dauphas and Rouxel, 2006; Busigny and Dauphas, 2007; Dauphas et al., 2009; Craddock and Dauphas, 2011). Accordingly, the precision is better than 0.06‰ for $\delta^{56}Fe$ and 0.12‰ for $\delta^{57}Fe$ (2 SD) for most samples. Since $\delta^{56}Fe$ and $\delta^{57}Fe$ data plot on a single mass-dependent fractionation line ($r^2 = 0.95$), only $\delta^{56}Fe$ values are discussed in this study.

4. RESULTS

4.1. General characteristics of the Seine River SPM

The water discharge varies from 26 to 807 m^3/s for the transect samples of the Seine River collected during the flood of February 22nd, 2006 and shows a clear increase with the distance from the Seine headwater to estuary (Table 2, and Chen et al., 2009a). The SPM content increases also downstream, from 17 mg/L for S29 to 122 mg/L for S37 at Meulan, with an exception for the near estuary sample S38 that has a SPM content of 57 mg/L (Fig. 2a), probably due to the coagulation effect caused by high salinity (Escoube et al., 2009). The samples collected in Paris over 3 years have water discharge ranging from 100 to 1013 m^3/s, with an average value of 380 m^3/s. In the following, waters collected in Paris with a discharge lower than this threshold is thus named low water samples, and vice versa. The concentration of SPM displays also a large variation, between 2 and 151 mg/L (average value of 37 mg/L), correlated to the water discharge ($n = 40$, $r^2 = 0.61$, see Supplementary Fig. S1). Low water samples in Paris have relatively low SPM contents (from 2 to 33 mg/L) compared to high water samples.

The mineralogy of suspended sediments in the Seine River is characterized by high content of carbonates (20–30%), occurring generally as relative large (i.e. >10 μm) crystals (Chen, 2008). Other mineral phases are essentially clay minerals (i.e. kaolinite, 25–40%) and quartz (20–40%). Organic matter and feldspars represent minor phases (<10%) and are usually present as fine particles (<10 μm). The proportion of sulfide mineral is low (<5%, Chen, 2008; Chen et al., 2009a). In general, the contents of carbonates and kaolinites increase with the water discharge. Samples of low water stage (mainly collected in summer) and downstream samples contain a relatively large amount of organic matter.

The concentration of POC varies from 27 to 75 mg/g for the basin-transect samples and shows an increase with the distance from the Seine spring, except for the two headwater samples S29 and S31 (Table 2). In Paris, POC content varies from 36 to 71 mg/g (with an average of 55 ± 12 mg/g) and shows a clear decrease with increasing water discharge ($y = -0.03x + 69.86$, $r^2 = 0.74$, $n = 11$, see Chen et al., 2009a). The high POC concentration in low water samples probably results from the presence of micro-algae such as diatoms (Chen et al., 2008). In general, anthropogenic samples also have high POC contents, up to 195 mg/g (Table 3; see also Chen et al., 2009a).

The granulometric mode is another interesting parameter allowing to describe the grain size distribution and the mineralogical nature of suspended sediments, while depending strongly upon the hydrodynamics of the river (Chen et al., 2009a; Bouchez et al., 2011). The distribution mode D_{90} (size below which 90% of the grains were found in a given sample) varies between 61 and 93 μm for basin-transect samples and displays a clear increase downstream (Fig. 2a). The temporal samples collected in Paris showed similar D_{90} variation (from 60 to 94 μm) and decreases with the water discharge (Chen, 2008). Suspended sediments with finer grain particles usually had lower carbonate contents and thus lower Ca/Al ratio. This provides an index of the relative abundance of clay minerals (fine grains) compared to carbonates (coarse grains) (Chen et al., 2009a).

4.2. Geochemical variations of the basin-transect samples

The concentrations of Na, Mg, Al, and K in SPM increase with the distance to the Seine spring for basin-transect samples, while Ca concentration decreases downstream to the estuary (Table 2). Iron concentration in SPM varies from 1.8 to 4.2 wt.% (respectively for samples S29 and S38) and displays an increase downstream along the basin-transect (Fig. 2b). Trace metals such as Cu, Zn, Pb and Ni that are readily impacted by human activities (Thévenot et al., 2007), show also similar

Table 2
Iron isotope compositions, element concentrations and organic matter contents in SPM and dissolved load of the Seine River.

		Discharge* (m^3/s)	SPM* mg/L	POC* mg/g	D_{90} μm	$\delta^{56}Fe_{SPM}$ ‰	Na_{SPM} wt.%	Mg_{SPM} wt.%	Al^*_{SPM} wt.%	K_{SPM} wt.%	Ca^*_{SPM} wt.%	Fe_{SPM} wt.%	Zn^*_{SPM} ppm	DOC ppm	$\delta^{56}Fe_{Dissolved}$ ‰	$Fe_{Dissolved}$ μmol/L
Samples of temporal series in Paris																
S1	23-12-04	413	53.6		94	0.04 ± 0.08	0.20	0.48	5.13	1.30	15.6	3.01	235	4.5		0.25
S2	21-01-05	336	6.3			0.03 ± 0.08	0.16	0.52	5.50	1.24	13.6	3.15	244	3.9		
S3	25-01-05	535	69.2				0.16	0.47	5.44	1.32	12.2	3.09	193	4.6		0.06
S4	27-01-05	436	81.4	57.1	80	0.03 ± 0.06	0.17	0.48	6.00	1.44	10.3	3.28	171	5.1		
S5	29-01-05	404	45.4				0.17	0.51	6.47	1.57	9.2	3.49	205	5.1		
S6	31-01-05	311	44.7				0.14	0.49	5.98	1.40	10.5	3.30	197	5.5		
S7	14-02-05	486	30.9				0.19	0.47	5.10	1.26	12.8	2.92	222	4.2		
S8	17-02-05	543	83		73		0.18	0.60	6.35	1.57	10.2	3.62	156	5.4		0.11
S9	20-02-05	542	73.4	42.2	78	0.04 ± 0.06	0.18	0.52	5.02	1.30	13.1	3.05	135	5.4	−0.21 ± 0.02	0.13
S10	22-02-05	483	60				0.18	0.48	4.55	1.22	14.4	2.77	130	5.6		0.03
S11	24-02-05	461	43.3				0.21	0.49	4.29	1.18	15.2	2.62	154	4.4		
S12	08-04-05	251	8.9			−0.05 ± 0.02	0.18	0.48	4.13	1.03	12.5	2.52	235	8.0		
S13	29-04-05	316	8.1				0.16	0.52	4.98	1.19	12.1	2.96	229	4.7		
S14	19-05-05	222	10.6			−0.02 ± 0.06	0.16	0.51	4.57	1.09	12.7	2.80	248	3.8		0.11
S15	25-05-05	180	5.5			0.01 ± 0.02	0.16	0.55	4.92	1.13	12.9	2.95	251	3.2		
S16	23-06-05	100	1.8			0.04 ± 0.08	0.17	0.59	4.86	1.10	12.3	3.05	378	3.7		
S17	11-07-05	179	21										444	10.9		
S18	25-07-05	119	14	58.3		0.03 ± 0.10	0.19	0.65	5.19	1.21	13.8	3.28	452	9.4		
S19	26-08-05	143	13.8	59.4		0.02 ± 0.06	0.17	0.69	4.81	1.10	13.8	3.09	403	3.4		0.02
S20	17-09-05	183	10.8	57.5		0.06 ± 0.08	0.18	0.64	4.55	1.06	13.0	2.97	358	5.9		0.04
S21	03-10-05	167	3.9			0.03 ± 0.12	0.16	0.59	4.45	1.01	12.2	2.86	356	6.3		0.11
S22	09-11-05	118	3.75											5.6		0.06
S23	29-11-05	122	3.2			0.03 ± 0.14	0.16	0.55	4.30	0.96	11.8	2.92	415	3.2		
S24	22-12-05	125	4.4	71.4		0.07 ± 0.12	0.16	0.57	5.54	1.18	9.9	3.56	330	2.5	−0.60 ± 0.04	0.14
S25	24-01-06	226	6.6	70.6		0.05 ± 0.06	0.18	0.49	4.66	0.98	10.5	2.80	291	2.9	−0.52 ± 0.04	0.08
S26	17-02-06	368	24.4										430	3.1		
S27	20-02-06	601	151	48.4	66	0.09 ± 0.08	0.12	0.51	6.15	1.25	10.2	3.41	243	4.3		0.09
S41	01-03-06	321	32.8										245	3.7		
S42	10-03-06	785	110		82	0.06 ± 0.08	0.15	0.50	5.53	1.19	12.8	3.09	223	3.9		0.03
S43	14-03-06	1,013	108	35.7		0.07 ± 0.06	0.13	0.45	5.36	1.11		3.10	195	5.0		
S44	20-03-06	730	36			0.06 ± 0.08	0.11	0.46	4.70	1.07	14.0	2.78	181	3.7		0.13
S45	31-03-06	775	46.4			0.09 ± 0.08	0.14	0.49	4.98	1.16	12.7	2.95	217	4.8		
S46	11-04-06	503	18										213	3.9		0.01
S47	15-05-06	379	11			0.05 ± 0.12	0.25	0.63	4.23	1.03	13.1	2.80	300	3.6		
S48	21-06-06	104	3.7											6.4		0.08
S63	13-10-06	294	33.8										291	5.6		0.09
S64	07-03-07	800	82.8	41.3	60	0.04 ± 0.06	0.17	0.55	6.12	1.42	11.9	3.60	244			0.02
S65	10-05-04	372	30.2	63.8	86	0.03 ± 0.06	0.17	0.46	3.84	0.92	11.8	2.26	290	4.3		0.09
Geographical transect of the sampling cruise of 22 Feb. 2006																
S28	S@Source(0#)													2.2		
S29	S@Bruncey(29)	25.5	17.2	56.1		0.09 ± 0.03	0.09	0.27	2.80	0.67		1.78	94	2.3		0.02
S30	S@Bar(98)	67.2	31.7	75		0.03 ± 0.03	0.06	0.34	2.89	0.69	22.0	1.98	123	2.4		
S31	Aube(188)	49	86	26.7		0.07 ± 0.03	0.11	0.54	5.73	1.19	15.0	3.29	116	7.2	0.00 ± 0.04	0.09
S32	S@Châtre(178)	31.7	62.8	35.3	61	0.08 ± 0.02	0.17	0.51	6.01	1.18	14.1	3.35	168	5.4	−0.10 ± 0.07	0.07
S33	S@Noyen(286)	96	102	29.5	61	0.05 ± 0.05	0.12	0.55	6.42	1.2	14.01	3.66	152	7.1	−0.19 ± 0.06	0.09
S34	Yonne	257	109		71		0.16	0.56	6.87	1.6	8.51	3.85	236	5.3		
S35	S@Fontaine(351)	400	106	44.9		0.05 ± 0.03	0.17	0.55	6.83	1.4	9.60	3.78	227	5.8	0.00 ± 0.04	0.08
S36	Oise	203	259		68		0.26	0.68	5.02	1.3	8.77	3.68	207	8.0		
S37	S@Meulun(514)	701	122	41.9	70	0.00 ± 0.03	0.22	0.70	5.98	1.4	9.21	3.87	263	7.1	−0.43 ± 0.04	0.11
S38	S@laBouille(689)	807	56.8	49.9	79	−0.01 ± 0.04	0.38	0.72	6.11	1.3		4.17	323	5.8	−0.25 ± 0.08	0.09
S39	Eure	27.1	47.6		93								330	4.5		
S40	Marne	157	116		61		0.17	0.68	5.19	1.2	13.62	3.27	162	4.2		

SPM, suspended particulate matter; Dissolved, dissolved load of the Seine River; POC, particulate organic carbon; DOC, dissolved organic carbon; D_{90}, the granulometric distribution mode, below which 90% of the grains were found in a given sample; Fe isotope analytical uncertainties correspond to external errors expressed as 2 standard deviation (2SD).

The distance to the Seine spring.

* Data from Chen et al. (2009a).

downstream increase, thus correlating with Fe concentration in SPM (Table 2). Iron isotope composition in SPM of basin-transect samples slightly decreases downstream from headwater to estuary, with $\delta^{56}Fe$ values ranging from

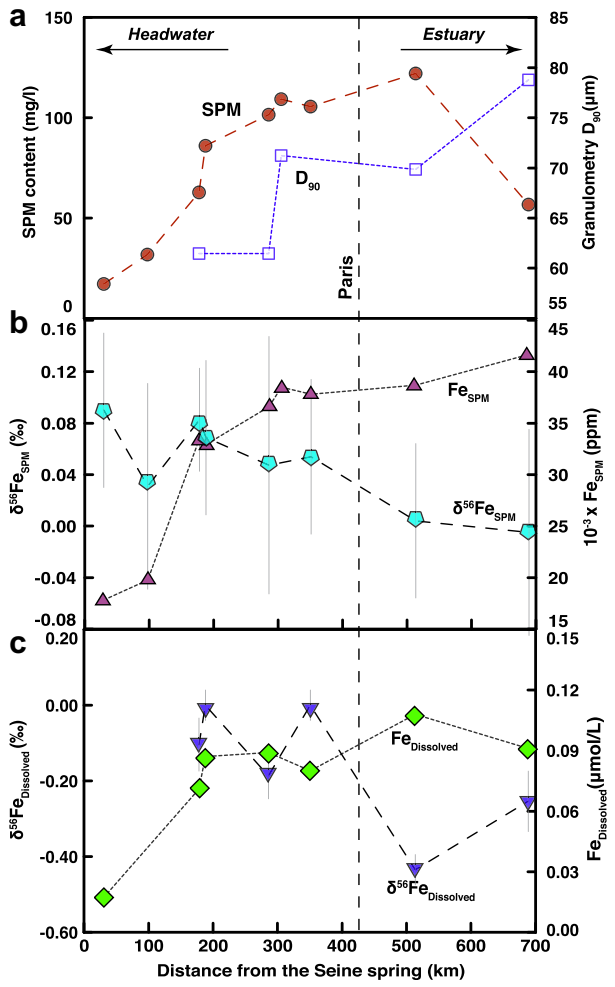

Fig. 2. Geographical variations of (a) SPM content and grain size distribution (D_{90}), (b) Fe concentration and isotopic composition in SPM, and (c) Fe concentration and $\delta^{56}Fe$ in dissolved load for basin-transect samples collected during the flood of February 22nd, 2006. Error bars are 2 standard deviations for $\delta^{56}Fe$ measurements.

0.09‰ to 0.00‰ and averaging 0.05‰ (Fig. 2b; Table 2). This small range of variation for $\delta^{56}Fe$ is consistent with the values reported for terrestrial clays and detrital silicate minerals (Beard et al., 2003; Poitrasson and Freydier, 2005; Dauphas and Rouxel, 2006).

In contrast, the dissolved load of the basin-transect samples displays larger $\delta^{56}Fe$ variation (from −0.44‰ to 0.06‰, Fig. 2c and Table 2), with the lowest values found near the estuary.

4.3. Temporal variations of samples in Paris

Particulate Fe (from 2.2 to 3.6 wt.%) and other major elements such as Na, Mg, Al, K and Ca in SPM of temporal series in Paris have similar concentration ranges as those of the basin-transect samples (Table 2). All samples, including the temporal series and basin-transect, show positive linear correlations between Fe/Ca molar ratio (here Ca normalization was used to eliminate carbonate dilution effect) and Na/Ca, Mg/Ca, K/Ca or Al/Ca ratios (Fig. 3). However, the plot of Fe/Al molar ratio vs. Ca concentration for temporal SPM samples shows an interesting trend: despite the carbonate dilution effect (parallel dispersion with the X-axis), the high water samples display a correlation between Fe/Al and Ca concentration (Fig. 4). This relationship can be probably explained by natural mixing of clay minerals with high Al content and heavy Fe-bearing minerals. The presence of heavy Fe-contained particles can be also confirmed by correlations between Fe (or Fe/Al ratio) and elements that are generally contained in heavy minerals such as Th, Cr and rare earth elements (Chen et al., 2009a). By contrast, SPM samples from low water stage in Paris do not follow this relationship and instead define a different trend (Fig. 4). These low water samples are thus characterized, at a given carbonate content, by much higher Fe enrichment compared to the high water stage sediments. Unlike major elements that do not display any correlation with the water discharge, concentrations of trace elements such as Cu, Zn, Pb and Ni decrease with increasing water discharge (Chen et al., 2009a). The $\delta^{56}Fe$ values of the Seine River SPM in Paris vary from −0.07‰ to 0.09‰ for the 3-year sampling period. Thus, the total $\delta^{56}Fe$ variation observed in the temporal series is almost twice that of the geographical variation on the Seine basin-transect. Like Fe concentration, $\delta^{56}Fe$ values do not display any correlation with water discharge. For the whole set of samples collected

Table 3
Iron concentrations and isotope compositions in headland rocks and SPM of anthropogenic samples.

Sample	Location	SPM mg/L	POC mg/g	$\delta^{56}Fe$ ‰	Fe wt.%
Headland bedrocks					
Chalk	Provins	29		0.24 ± 0.08	0.9
Granite	Morvan	30		0.17 ± 0.06	1.2
Potential anthropogenic samples					
RF5	Roof streaming		113	0.16 ± 0.04	1.8
RD1	Road streaming		235	−0.00 ± 0.06	1.7
SW1	Noisy-le-Grand	336		−0.01 ± 0.08	0.1
PTWW1	Noisy-le-Grand	49	263	0.00 ± 0.08	0.4
PTWW2	Achères	28	195	0.15 ± 0.04	10.6

SPM, suspended particulate matter; POC, particulate organic carbon; analytical uncertainties on $\delta^{56}Fe$ values are external errors expressed as 2 standard deviation (2SD).

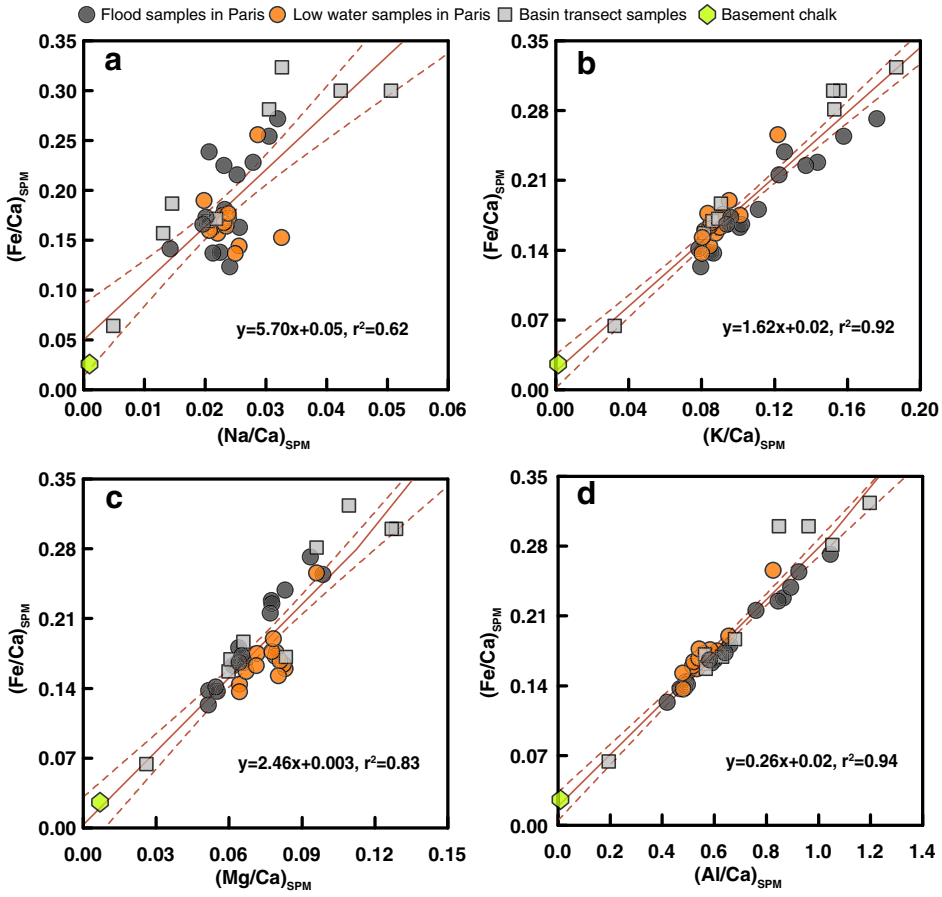

Fig. 3. Relationships between the molar ratios of Fe/Ca and Na/Ca (a), K/Ca (b), Mg/Ca (c) and Al/Ca (d) for geographical transect SPM samples (squares) of the Seine basin, and temporal samples collected during flood (dark-grey points) and low water period (orange points) in Paris. The headland chalk (hexagon) is also showed in the figures for comparison. These correlations demonstrate that Fe is mainly carried by clay minerals since Al, K, Mg and Na are their main constituents. Dashed lines represent the error ellipse on the fit of data points at 95% confidence level. (For interpretation of the references to color in this figure legend, the reader is referred to the web version of this article.)

both in Paris and the Seine basin, δ^{56}Fe values of the suspended sediments display a poor correlation with Al/Fe molar ratio (Fig. 5a) and δ^{66}Zn values (Fig. 5b) reported in Chen et al. (2009a).

Compared with the SPM, the dissolved load shows relatively lower δ^{56}Fe, with values of −0.21‰, −0.52‰ and −0.60‰ for the high water sample S9, and the low water samples S24 and S25, respectively (Table 2).

4.4. Bedrocks and anthropogenic samples

The headland chalk and granite have Fe concentrations of 0.87 and 1.14 wt.%, respectively (Table 3). Compared with the Seine SPM, their δ^{56}Fe values are relatively high, being +0.24‰ and +0.17‰ for chalk and granite, respectively. SPM of potential anthropogenic samples have Fe contents varying from 0.09 to 10.57 wt.%, with an average value of 2.91 wt.%, higher than that of the bedrocks (average ~1.01 wt.%, Table 3). These samples have δ^{56}Fe values from −0.01‰ to +0.14‰, similar to the range of the Seine SPM (from −0.05‰ to +0.09‰, Table 3).

5. DISCUSSION

5.1. Distribution of iron between particulate and dissolved loads

In the Seine River, Fe is contained in both dissolved and particulate loads. The fractions of particulate and dissolved Fe (Fe_{part}% and Fe_{diss}%) relative to total Fe were calculated for each sample as follow:

$$Fe_{part}\% = 1 - Fe_{diss}\% = [SPM] \times C^{Fe}_{SPM} / ([SPM] \times C^{Fe}_{SPM} + C^{Fe}_{diss}) \quad (3)$$

where [SPM], C^{Fe}_{SPM} and C^{Fe}_{diss} represent the SPM content (mg/L), Fe concentrations in SPM (μg/mg) and dissolved loads (μg/L), respectively. The fraction of dissolved Fe calculated using Eq. (3) is between 0.04% and 5.22% of the total Fe, and averages 0.89% ($n = 27$, Table 2). Suspended particulate matter (SPM) contains between 94.78% and 99.96% of the total Fe, with an average of 99.11% ($n = 24$). The small variations of the distribution of Fe between these two phases are related to water discharge, and

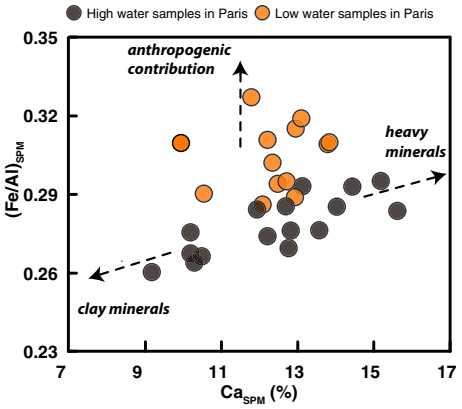

Fig. 4. Relationship between Fe/Al molar ratio and Ca concentration in SPM. In addition to the carbonate dilution effect, the slight increase of Fe/Al with Ca for high water samples (dark-grey points) suggests the presence of heavy Fe-bearing minerals (such as magnetite or hematite) in SPM. The deviation of low water samples (orange points) from the flood trend probably results from the anthropogenic contribution. (For interpretation of the references to color in this figure legend, the reader is referred to the web version of this article.)

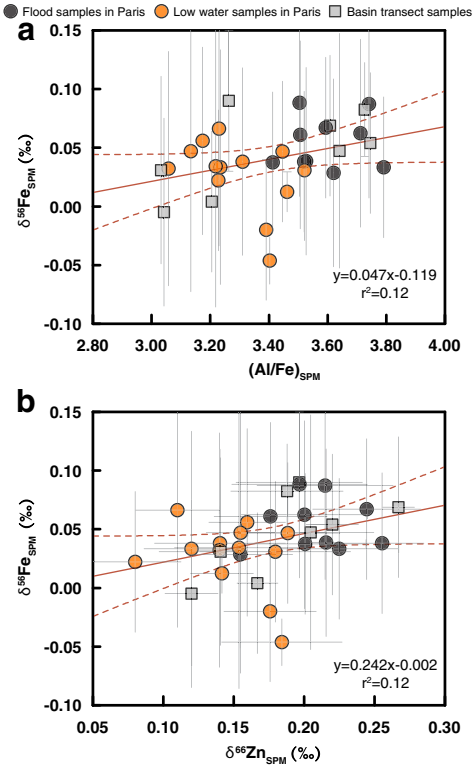

Fig. 5. Suspended particulate matter δ^{56}Fe versus (a) Al/Fe molar ratio and (b) δ^{66}Zn, (from Chen et al., 2009a) for both basin-transect (squares) and Paris temporal (round points) samples. Contrasting with large δ^{66}Zn variations, δ^{56}Fe values in SPM remains nearly constant (b). The analysis of bedrocks and anthropogenic samples confirms the similarity of δ^{56}Fe values between natural and anthropogenic sources. Error bars are 2 standard deviations for δ^{56}Fe measurements.

more specifically to total SPM load. Indeed, an increase in the water discharge induces an increase in the SPM load, and enhances the fraction of Fe contained in the particles. This is well illustrated by the plot of the Fe fraction in SPM versus total SPM load (Fig. 6) and well explained by the fact that Fe concentration in SPM is less variable (2 times) compared to the SPM content (80 times, Table 2). In Paris, the samples collected during high water discharge show larger SPM content and higher Fe fraction in SPM than those collected during low water discharge. Similar conclusions can be drawn from the samples collected along the basin-transect, since water discharge increases downstream.

The average proportions of particulate Fe transferred to the ocean can be estimated using the long-term monitoring of SPM in the Seine River (average SPM of 44 mg/L from 1959 to 1994; Roy et al., 1999) and the relation between Fe_{part}% and SPM load (Fig. 6). We find that about 99% of the Fe transferred to the ocean is contained in the SPM, in good agreement with the average value obtained from dataset in Table 2 (i.e. 99.11%). The main flux of Fe from the Seine River to the ocean is thus carried by suspended matter rather than dissolved species. This highlights the importance of studying SPM to assess first order information about the global biogeochemical cycles of Fe and its isotopes.

5.2. Iron in suspended particulate matter

5.2.1. Evidence for an anthropogenic iron input

A mean of estimating the anthropogenic contribution to the Fe budget is to determine the enrichment factor (EF). The enrichment factor is calculated as a normalization of Fe concentration to that of an element mainly derived from natural sources (e.g. Al, Th, Ti). It provides an index of Fe enrichment relative to natural background. This normalization eliminates any dilution effect due to increase in natural components such as quartz, carbonate or organic matter, and allows a better comparison of the relative Fe concentrations among the different samples than absolute Fe

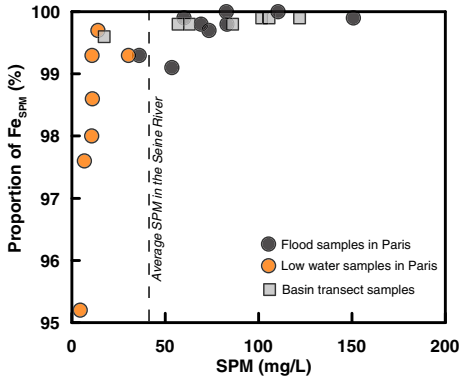

Fig. 6. Relation between the proportion (in %) of Fe transported in SPM and the SPM content. Dissolved Fe represents only a small fraction of the total Fe (with an average value of 0.89%), highlighting the importance of studying SPM to access the global biogeological cycle of Fe and its isotopes.

concentrations. In this study, the Fe enrichment factor EF(Fe) was calculated using Al for normalization as:

$$EF(Fe) = (Fe/Al)_{sample}/(Fe/Al)_{bkg} \quad (4)$$

where "bkg" denotes the natural background. EF(Fe) = 1 indicates that Fe is similar to natural background while EF(Fe) > 1 corresponds to a Fe enrichment (relative to Al). The choice of reference reservoir as the natural background is critical. Here we take the molar ratio $(Fe/Al)_{bkg}$ ~ 0.21 reported in Thévenot et al. (2002, 2007) for the background composition in the Seine basin, based on the chemical composition of fluvial pre-historical (3500 BP; Thévenot et al., 2007) and headwater sediments. This value is identical within uncertainty to the molar ratio Fe/Al (0.22) of the Post Archean Shale Composition (PASC) taken as representative of sedimentary silicates (Taylor and McLennan, 1995), or that (between 0.22 and 0.26) found in sediments of the Mackenzie River that drains mainly sedimentary rocks (Dellinger M., personal communication). EF(Fe) calculated for SPM of the Seine River ranges between 1.24 and 1.68, with an average of 1.39 ± 0.20 (2SD, $n = 42$), indicating that all samples are slightly enriched in Fe relative to natural background. In Paris, low water samples display generally higher EFs (from 1.36 to 1.68) compared to the high water samples (1.24 to 1.40). Along the upstream–downstream transect, EF(Fe) values are mostly around 1.30 upstream Paris city, then show a large range of variation for samples in Paris (1.26 to 1.56), and finally display only high values downstream (1.49 to 1.57). In comparison to Zn, the Fe enrichment is moderate since EF(Zn) relative to Al was shown to reach values up to 5.3, observed in Paris during low water stages (Chen et al., 2009a). This difference in Fe and Zn enrichment factors indicates that Zn is more sensitive to anthropogenic processes.

In addition to source contribution, processes such as the adsorption, precipitation and coagulation can transfer dissolved Fe into particulate matter (Teutsch et al., 2005). Since Fe in the Seine River is mainly in particulate form (average proportion of 99%), this transfer would be very limited. This is also confirmed by the calculation of Fe isotope fractionation upon Fe adsorption or precipitation (Appendix A). Thus, the increase of EFs along the upstream–downstream transect in the Seine River results from an anthropogenic Fe contribution, which occurs mainly at Paris mega-city. The anthropogenic Fe contribution seems even more important considering that the amount of SPM also increases downstream (Fig. 2a).

In fact, the most convincing argument in favor of an anthropogenic impact on Fe data is the positive correlation between Fe/Al and Zn/Al ratios (Fig. 7a). Zn is known to be largely affected by anthropogenic activities in the Seine River (Meybeck et al., 2007; Thévenot et al., 2007; Chen et al., 2008, 2009a,b; Priadi et al., 2012). In a previous paper, Zn isotope composition of SPM in the Seine River was used as a tracer of human activity, with natural $\delta^{66}Zn$ values around 0.35‰ being progressively lowered due to anthropogenic input down to 0.08‰ (Chen et al., 2009a). Fig. 7b illustrates that $\delta^{66}Zn$ values of SPM are negatively correlated with Fe/Al ratio. Once again, this correlation supports the idea of an anthropogenic source for Fe in SPM. Iron concentration and Zn isotope composition can thus be coupled to trace metal contamination in river systems.

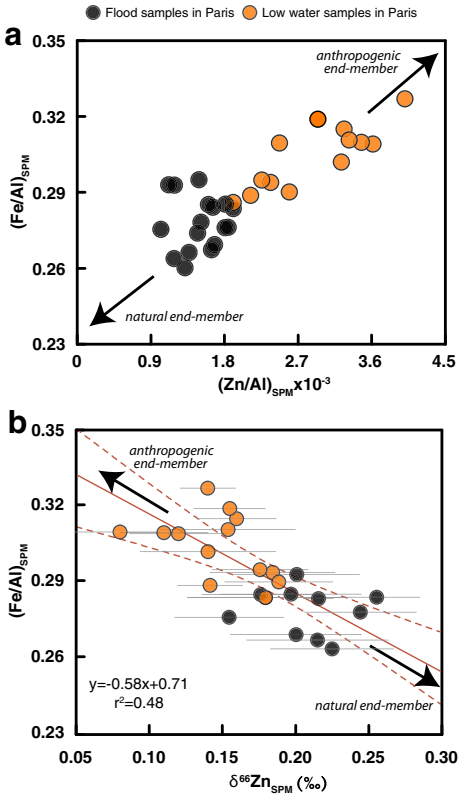

Fig. 7. Linear relationships between Fe/Al and (a) Zn/Al molar ratios and (b) $\delta^{66}Zn$ (from Chen et al., 2009a) in SPM samples. The low water samples (orange points) are enriched in Fe, Zn and lighter Zn isotopes, and well distinguishable from flood samples (dark-grey points). These correlations indicate a mixing between natural and anthropogenic sources to SPM Fe in the Seine River. (For interpretation of the references to color in this figure legend, the reader is referred to the web version of this article.)

5.2.2. Characterizing the natural and anthropogenic sources

The correlations observed between Fe and Zn in SPM (Fig. 7) likely represent mixing between natural and anthropogenic contributions. Natural Fe may be derived from carbonates. Fig. 3d illustrates that Al/Ca ratio of ~0 corresponds to Fe/Ca ratio of 0.02. This value is similar to Fe/Ca ratio of the chalk sample analyzed herein (Fe/Ca of 0.03), suggesting that a small part of the total Fe in the SPM is present in the carbonates. Considering that all Ca in SPM is derived from carbonates, we calculate that the maximum contribution of carbonates to Fe budget in Seine SPM is 23%. The natural sources contain thus other Fe-bearing mineral phases. In fact, Fe in the Seine SPM is mainly carried by weathered materials derived from surficial sedimentary minerals, soils and loess, including iron-rich soils which are inherited from human activities (i.e. mining, exploitation and war) in the Tertiary. These natural materials are mostly composed of clay minerals, as demonstrated by XRD and SEM analyses (Chen et al., 2009a),

and the linear correlations between Fe and Na, Mg, K and Al concentrations (Fig. 3). Moreover, the slight increase in Fe/Al ratio for high water samples with Ca concentration (Fig. 4) also supports the presence of Fe-enriched heavy minerals such as Fe-oxides (hematite Fe_2O_3 and magnetite Fe_3O_4) or Fe-hydroxides (goethite FeOOH). However, given the clear correlation between Fe and Al (also K and Mg, Fig. 3), these heavy minerals likely present a small proportion of total Fe budget.

We attempted to estimate the Fe isotope composition of potential natural sources by two different methods: (1) analysis of bedrocks (headland granite and chalk), and (2) geochemical trends. Iron isotope compositions of bedrocks are significantly enriched in heavy isotopes (with δ^{56}Fe values of +0.17‰ and +0.24‰ for granite and chalk, respectively; Table 3) compared to SPM in the headwater (δ^{56}Fe ~0.10‰). The origin of distinct Fe isotope compositions between our bedrock samples and SPM is not clear. Although the data are scarce, Matthews et al. (2004) demonstrated that limestone and marls have variable Fe isotope compositions (−0.12‰ to +0.33‰). The granitic rocks also show large δ^{56}Fe variation (Poitrasson and Freydier, 2005). As weathering processes preferentially release light Fe isotopes, resulting in an enrichment of heavy isotope in the residue (Fantle and DePaolo, 2004; Yesavage et al., 2012), this isotopic contrast may imply that SPM is not directly derived from the bedrocks but from the weathered products with relatively light Fe isotopes.

The Fe isotope composition of the natural source can also be roughly estimated using geochemical trends between δ^{56}Fe values and other parameters such as Al/Fe ratio or δ^{66}Zn (Figs. 5 and 7). In these diagrams, mixing between two end-members (e.g. natural versus anthropogenic) should define a straight line. Considering the natural end-member has δ^{66}Zn of +0.35‰ (Chen et al., 2009a), the calculated Fe/Al molar ratio is about 0.238 and the corresponding δ^{56}Fe value of ~0.08‰ for the natural Fe sources according to the relationships in Figs. 5 and 7. Interestingly, this value is consistent with δ^{56}Fe of the headwater sample S29 (0.09‰), and the average value (0.07‰) for the upper continental crust (Poitrasson, 2006) and most SPM of the Amazon River system (dos Santos Pinheiro et al., 2013). We conclude that the natural sources for the SPM of the Seine River are likely dominated by clay minerals, with minor amount of carbonates and heavy minerals, and have a δ^{56}Fe value of ~0.10‰.

Unlike natural sources, anthropogenic contribution to SPM cannot be easily characterized from chemical and isotopic analyses. In big cities such as Paris conurbation, a large part of the anthropogenic Fe may be derived from the sewer systems. Although the existence of various metal oxides, silicates and other metal particles such as stainless steel fragments were evidenced (El Samrani et al., 2004; Franke et al., 2009), the sewer sediment or SPM are substantially enriched in sulfide minerals, representing up to ~40% of heavy metal carriers (Houhou et al., 2009; Priadi et al., 2012). In addition to sulfides, anthropogenic input may also be characterized by high concentration of Fe-bearing organic matter (Table 2; Rocher et al., 2004; Chen et al., 2009a).

Importantly, all low water samples display different geochemistry from other suspended sediments of the Seine River (Figs. 4, 5 and 7). For instance, in diagram of Fe/Al vs Ca concentration (Fig. 4), SPM of low water samples are enriched in Fe relative to high water samples, probably due to variable contributions of anthropogenic sources. This trend is also obvious in plot of Fe/Al vs. Zn/Al or δ^{66}Zn (Fig. 7), where low water samples are enriched in both Zn and Fe compared to SPM samples at high water stage. Previous study on Zn isotopes showed that the anthropogenic contribution increase from high to low water discharge, even up to 100% for some low water samples (Chen et al., 2009a). The relationships illustrated in these diagrams indicate thus an overwhelming contribution of anthropogenic sources at low water stages.

In the present work, various anthropogenic samples from the Seine basin, including roof runoff, road runoff, untreated and plant-treated wastewaters, show a limited range of δ^{56}Fe values, from −0.01‰ to 0.14‰ (Table 3). This range is similar to that determined for the Seine SPM, and overlaps the value defined for the natural contribution (~0.10‰). The data are thus self-consistent and support that Fe isotope composition of SPM samples may reflect a mixing between natural and anthropogenic Fe sources. However, the similarity between these two sources precludes any precise quantification of their contribution to SPM using only Fe isotopes. Similarly to the natural sources, the mean Fe isotope composition of the anthropogenic end-member can be roughly estimated using the correlations in Figs. 5 and 7. Assuming a δ^{66}Zn value of 0.08‰ for the anthropogenic sources (Chen et al., 2009a), the calculation gives a corresponding δ^{56}Fe value of 0‰.

5.3. Iron in the dissolved load

The dissolved Fe concentration (<0.2 μm) measured in the Seine samples varies from 0.008 to 0.247 μmol/L (average = 0.083 ± 0.1 μM, 2SD, $n = 27$, Table 2). These values are significantly high considering the very low solubility of Fe in oxygenated aqueous fluids and for instance, in comparison to Fe concentration in the open ocean (0.1–1 nM Fe; Lacan et al., 2008). This implies that dissolved Fe is largely in colloidal form, as suggested in previous studies on river waters for filtrated fractions of increasing pore-size (Benoit and Rozan, 1999; Pokrovsky and Schott, 2002; Ilina et al., 2013). These colloidal forms may include Fe-oxides, clays, sulfides, and high molecular weight organic compounds (Buffle and Leppard, 1995; Lyven et al., 2003). The speciation of dissolved Fe in the Seine River cannot be clearly delineated from data of the present study. The linear relationship between δ^{56}Fe and DOC/Fe of the dissolved load (Fig. 8a) likely reflects a mixing between two end-members: one enriched in heavy Fe isotopes and in organic carbon (with high DOC/Fe), and the other characterized by low δ^{56}Fe and DOC/Fe. The end-member with high δ^{56}Fe values may represent Fe associated with organic matter. In contrast, Fe-rich (C-poor) end-member probably corresponds to other phases such as Fe-oxyhydroxide or sulfide colloids. These results are consistent with recent findings on boreal and temperate rivers, showing that

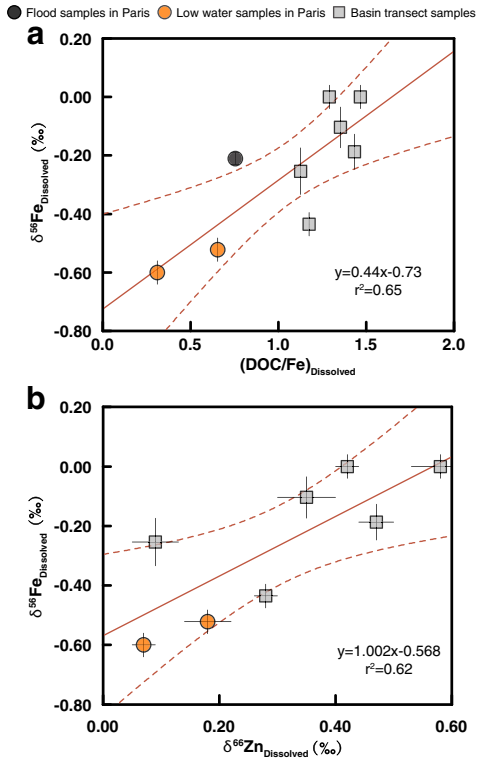

Fig. 8. Relationships between δ^{56}Fe and (a) DOC/Fe and (b) δ^{66}Zn for the dissolved load. The linear relationships likely reflect a mixing of two end-members. Dissolved Fe of natural origin is mainly associated with organic colloids, while anthropogenically-derived Fe may be transported in other forms such as sulfides, or Fe-oxyhydroxides. Error bars are 2 standard deviations for δ^{56}Fe measurements.

Fe-poor, C-rich colloids exhibit stronger enrichments in heavy isotopes than associated Fe-rich, C-poor colloids (Ilina et al., 2013).

Similarly to SPM, the dissolved Fe enrichment due to anthropogenic contribution was investigated by the relationships with Zn, which is more strongly impacted by human activities (Meybeck et al., 2007; Thévenot et al., 2007; Chen et al., 2008, 2009a,b; Priadi et al., 2012). Unlike the poor relationship found in SPM (Fig. 5b), the dissolved load displays a clear correlation between δ^{56}Fe and δ^{66}Zn (Fig. 8b). A previous study has demonstrated that δ^{66}Zn values in the dissolved load of the Seine River reflect various proportions of anthropogenic (i.e. −0.04‰) versus natural input (i.e. 0.88‰) (Chen et al., 2008). Thus the correlation in Fig. 8b may imply that dissolved Fe is also derived from a mixing of these two sources, with the lowest δ^{56}Fe values (i.e. −0.60‰) corresponding to the largest anthropogenic contribution (Fig. 8). In this case, the natural source should have relatively high δ^{56}Fe value (i.e. >0.00‰). Coupling this finding with δ^{56}Fe-DOC/Fe relationship (Fig. 8a), we can propose that dissolved Fe in natural end-member is likely carried by colloidal organic matters. The Fe derived from anthropogenic sources may be in the form of Fe-oxyhydroxide or sulfide colloids. Most terrestrial Fe(III) oxides and hydroxides precipitating from either biotic or abiotic pathways are enriched in heavy isotopes as shown by experimental studies (Bullen et al., 2001; Skulan et al., 2002; Beard and Johnson, 2004; Balci et al., 2006) and data on natural samples such as riverine Fe-oxyhydroxide colloids (Ingri et al., 2006). In contrast, pyrites from modern and ancient sediments are mostly characterized by negative δ^{56}Fe values (Rouxel et al., 2005; Guilbaud et al., 2011). Pyrites from modern marine sediments at two sites along the California continental margin were found relatively homogeneous in terms of δ^{56}Fe values (−0.70 ± 0.20‰; Severmann et al., 2006). Pyrite nodules from the upper Jurassic Kimmeridge formation of Dorset (United Kingdom) show a small range of δ^{56}Fe values between −0.30‰ and −0.21‰ (Matthews et al., 2004). Pyrites from Archean rocks show the largest range of Fe isotope variation ever observed on Earth's samples over geological time with the most negative δ^{56}Fe values down to −3.5‰ (Anbar et al., 2005; Rouxel et al., 2005; Archer and Vance, 2006). Based on these literature data, we suggest that the negative δ^{56}Fe values (down to −0.60‰) measured in the dissolved load of the Seine River are thus more compatible with anthropogenic Fe sulfide than Fe-oxyhydroxide colloids. This is also in good agreement with a recent mineralogical study on the Seine River particulate matters (Priadi et al., 2012). Yet, the origin of anthropogenic contribution to dissolved Fe remains unknown. More work is thus needed to systematically investigate the possible contributing sources.

6. CONCLUSIONS AND PERSPECTIVES

The Seine River drains a basin strongly impacted by human activities. The present study shows for the first time the impact of anthropogenic processes on Fe isotope transfer to the ocean through river systems. In the Seine River, 99% of the Fe transferred to the ocean is contained in the SPM. Relations between Fe and Zn evidence a substantial anthropogenic Fe input to SPM. The calculation of SPM Fe enrichment factors (relative to Al) shows that Fe is increased up to 68% and on average by 39% relative to the natural background. Contrasting with large Zn isotope variations, Fe isotope compositions in SPM remain nearly constant (from −0.05‰ to 0.09‰). The transfer of dissolved Fe to SPM thus has a limited effect on SPM δ^{56}Fe values. This implies that anthropogenic sources likely have similar Fe isotope composition to the natural background. Compared to the small δ^{56}Fe range determined in SPM, δ^{56}Fe values of dissolved load shows a significant variation from −0.60‰ to 0.06‰, and a linear correlation with δ^{66}Zn (data from Chen et al., 2008). This linear relationship indicates that δ^{56}Fe variation in the dissolved load results from a mixing between anthropogenic and natural end-members, enriched in light and heavy isotopes, respectively. Moreover, the positive correlation between δ^{56}Fe and DOC/Fe ratio of the dissolved load suggests that dissolved Fe of natural origin is mainly associated with organic colloids, while anthropogenically-derived Fe may be transported in other forms such as sulfide colloids. Compared to SPM, the larger δ^{56}Fe variations observed in the dissolved load are more promising for tracing anthropogenic

contributions to natural river systems. As a result, our study demonstrates that Fe concentration and isotope composition can be coupled with Zn isotope data to trace natural and anthropogenic sources of Fe in river system. The anthropogenic Fe input will fertilizer the ocean and increase the primary productivity of phytoplankton, and thus may ultimately impact the global carbon cycle and the corresponding climate change.

Our work on the Seine River has also implications for global Fe cycling to the modern oceans, since many rivers (e.g., Scheldt, St-Laurence) in the world are presently impacted by human activities (Foster and Charlesworth, 1996; Gaillardet et al., 1999; Zwolsman and van Eck, 1999). Although the natural Fe flux is increased up to 39% after anthropogenic input, the Fe isotope composition in SPM is not changed by more than 0.10‰ and is still very similar to average detrital sediments (Beard et al., 2003; Beard and Johnson, 2004). It suggests that Fe-polluted rivers carry an isotope signature essentially indistinguishable from the natural detrital Fe flux. Natural reactions related to redox change in soils and rivers, together with organic matter complexation, may produce more important variations in the isotope composition of particulate Fe transferred by rivers to the ocean compared to anthropogenic impact (Fantle and DePaolo, 2004; Bergquist and Boyle, 2006). Compared to SPM, the fluxes of dissolved Fe with low δ^{56}Fe values may display stronger impact on Fe and its isotopes in ocean, given the fact that the flocculation in estuaries does not modify significantly Fe isotope composition of the dissolved pool (Escoube et al., 2009). As a result, the overall fluxes of Fe to the ocean have generally low δ^{56}Fe values (<0.10‰), as shown by studies on continental rivers (Fantle and DePaolo, 2004; Bergquist and Boyle, 2006), on benthic Fe from marine sediments (Homoky et al., 2009; Severmann et al., 2010), on hydrothermal systems (Sharma et al., 2001; Severmann et al., 2004; Rouxel et al., 2008), and on atmospheric particles (Beard et al., 2003). An intriguing question is the origin of the distinctive Fe isotope signatures observed between (1) theses main sources of Fe input to the oceans, with generally negative δ^{56}Fe values, and (2) Fe dissolved in the Pacific Ocean, with positive δ^{56}Fe values between 0.00‰ and +0.60‰ (similar to particulate matter, Radic et al., 2011). According to our results, the anthropogenic contribution is not able to explain this discrepancy. The positive δ^{56}Fe values found in the Pacific Ocean requires a Fe flux, enriched in light isotopes, output from the dissolved reservoir in the ocean. Biological uptake by phytoplankton in the upper ocean regions is the most likely mechanism triggering this effect (Radic et al., 2011), as demonstrated by similar results of preferential uptake of light Fe isotopes by higher plants (Guelke and von Blanckenburg, 2007; Guelke et al., 2010). However, experimental results show that metal uptake by diazotroph bacteria favors heavy isotopes during biological assimilation, thus resulting in an enrichment of light isotopes in the residual dissolved Fe (Wasylenki et al., 2007). These contrasting Fe isotope variations need to be clarified by further studies on Fe isotope fractionation associated with various assimilation pathways.

ACKNOWLEDGMENTS

We thank J.-L. Birck, J. Bouchez, G. Morin from IPGP for discussion, M. Tharaud from Université Paris-Diderot, O. Beyssac and N. Findling from Ecole Normale Supérieur and S. Huon from Université Pierre & Marie Curie for analytical assistance and constructive discussions. J.-B. Chen was financially supported by the Region Ile-de-France, SKLEG and "hundred talents" project of the Chinese Academy of Sciences. This is IPGP contribution n°3463.

APPENDIX A. SUPPLEMENTARY DATA

Supplementary data associated with this article can be found, in the online version, at http://dx.doi.org/10.1016/j.gca.2013.12.017.

REFERENCES

Albarède F. and Beard B. L. (2004) Analytical methods for non-traditional isotopes. In *Geochemistry of Non-traditional Stable Isotopes* (eds. C. M. Johnson, B. L. Beard and F. Albarède). Mineralogical Society of America and Geochemical Society, Washington, DC, pp. 113–152.

Anbar A. D. and Knoll A. H. (2002) Proterozoic ocean chemistry and evolution: a bioinorganic bridge? *Science* **297**, 1137–1142.

Anbar A. D., Jarzecki A. A. and Spiro T. G. (2005) Theoretical investigation of iron isotope fractionation between $Fe(H_2O)_6^{3+}$ and $Fe(H_2O)_6^{2+}$: implications for iron stable isotope geochemistry. *Geochim. Cosmochim. Acta* **69**, 825–837.

Archer C. and Vance D. (2006) Coupled Fe and S isotope evidence for Archean microbial Fe(III) and sulfate reduction. *Geology* **34**, 153–156.

Balci N., Bullen T. D., Witte-Lien K., Shanks W. C., Motelica M. and Mandernack K. W. (2006) Iron isotope fractionation during microbially stimulated Fe(II) oxidation and Fe(III) precipitation. *Geochim. Cosmochim. Acta* **70**, 622–639.

Beard B. L. and Johnson C. M. (1999) High precision iron isotope measurements of terrestrial and lunar materials. *Geochim. Cosmochim. Acta* **63**, 1653–1660.

Beard B. L. and Johnson C. M. (2004) Fe isotope variations in the modern and ancient Earth and other planetary bodies. In *Geochemistry of Non-traditional Stable Isotopes* (eds. C. M. Johnson, B. L. Beard and F. Albarède). Mineralogical Society of America and Geochemical Society, Washington, DC, pp. 319–357.

Beard B. L., Johnson C. M., Skulan J. L., Nealson K. H., Cox L. and Sun H. (2003) Application of Fe isotopes to tracing the geochemical and biological cycling of Fe. *Chem. Geol.* **195**, 87–117.

Belshaw N. S., Zhu X. K. and O'Nions R. K. (2000) High precision measurement of iron isotopes by plasma source mass spectrometry. *Int. J. Mass Spectrom.* **197**, 191–195.

Benoit G. and Rozan T. F. (1999) The influence of size distribution on the particle concentration effect and trace metal partitioning in rivers. *Geochim. Cosmochim. Acta* **63**, 113–127.

Bergquist B. A. and Boyle E. A. (2006) Iron isotopes in the Amazon river system: weathering and transport signatures. *Earth Planet. Sci. Lett.* **248**, 54–68.

Blain S., Queguiner B., Armand L., Belviso S., Bombled B., Bopp L., Bowie A., Brunet C., Brussaard C., Carlotti F., Christaki U., Corbiere A., Durand I., Ebersbach F., Fuda J.-L., Garcia N., Gerringa L., Griffiths B., Guigue C., Guillerm C., Jacquet S., Jeandel C., Laan P., Lefevre D., Lo Monaco C., Malits A.,

Mosseri T., Obernosterer I., Park Y.-H., Picheral M., Pondaven P., Remenyi T., Sandroni V., Sarthou G., Savoye N., Scouarnec L., Souhaut M., Thuiller D., Timmermans K., Trull T., Uitz J., van Beek P., Veldhuis M., Vincent D., Viollier E., Vong L. and Wagener T. (2007) Effect of natural iron fertilization on carbon sequestration in the Southern Ocean. *Nature* **446**, 1070–U1071.

Bouchez J., Gaillardet J., France-Lanord C., Maurice L. and Dutra-Maia P. (2011) Grain size control of river suspended sediment geochemistry: clues from Amazon River depth profiles. *Geochem. Geophys. Geosyst.* **12**, 1029. http://dx.doi.org/10.1029/2010GC003380.

Brantley S. L., Liermann L. and Bullen T. D. (2001) Fractionation of Fe isotopes by soil microbes and organic acids. *Geology* **29**, 535–538.

Brantley S. L., Liermann L. J., Guynn R. L., Anbar A., Icopini G. A. and Barling J. (2004) Fe isotopic fractionation during mineral dissolution with and without bacteria. *Geochim. Cosmochim. Acta* **68**, 3189–3204.

Buffle J. and Leppard G. G. (1995) Characterization of aquatic colloids and macromolecules: 2. Key role of physical structures on analytical results. *Environ. Sci. Technol.* **29**, 2176–2184.

Bullen T. D., White A. F., Childs C. W., Vivit D. V. and Schulz M. S. (2001) Demonstration of significant abiotic iron isotope fractionation in nature. *Geology* **29**, 699–702.

Busigny V. and Dauphas N. (2007) Tracing paleofluid circulations using iron isotopes: a study of hematite and goethite concretions from the Navajo Sandstone (Utah, USA). *Earth Planet. Sci. Lett.* **254**, 272–287.

Butler I. B., Archer C., Vance D., Oldroyd A. and Rickard D. (2005) Fe isotope fractionation on FeS formation in ambient aqueous solution. *Earth Planet. Sci. Lett.* **236**, 430–442.

Chen J.- B. (2008) La contamination métallique de la Seine et des rivières de son bassin: traçage par les isotopes du Zinc. Ph. D. thesis, Université Paris 7, Institut de Physique du Globe de Paris, 202.

Chen J.-B., Gaillardet J. and Louvat P. (2008) Zinc isotopes in the Seine River waters, France: a probe of anthropogenic contamination. *Environ. Sci. Technol.* **42**, 6494–6501.

Chen J.-B., Gaillardet J., Louvat P. and Huon S. (2009a) Zn isotopes in the suspended load of the Seine River, France: isotopic variations and source determination. *Geochim. Cosmochim. Acta* **73**, 4060–4076.

Chen J.-B., Louvat P., Gaillardet J. and Birck J.-L. (2009b) Direct separation of Zn from dilute aqueous solutions for isotope composition determination using multi-collector ICP-MS. *Chem. Geol.* **259**, 120–130.

Chetelat B. and Gaillardet J. (2005) Boron isotopes in the Seine River, France: a probe of anthropogenic contamination. *Environ. Sci. Technol.* **39**, 2486–2493.

Craddock P. R. and Dauphas N. (2011) Iron isotopic compositions of geological reference materials and chrondrites. *Geostand. Geoanal. Res.* **35**, 101–123.

Crosby H. A., Johnson C. M., Roden E. E. and Beard B. L. (2005) Coupled Fe(II)–Fe(III) electron and atom exchange as a mechanism for Fe isotope fractionation during dissimilatory iron oxide reduction. *Environ. Sci. Technol.* **39**, 6698–6704.

Dauphas N. and Rouxel O. J. (2006) Mass spectrometry and natural variations of iron isotopes. *Mass. Spectrom. Rev.* **25**, 515–550.

Dauphas N., Janney P. E. and Mendybaev R. A. (2004) Chromatographic separation and multicollection-ICPMS analysis of iron. Investigating mass-dependent and mass-independent isotope effects. *Anal. Chem.* **76**, 5855–5863.

Dauphas N., Pourmand A. and Teng F.-Z. (2009) Routine isotopic analysis of iron by HR-MC-ICPMS: how precise and how accurate? *Chem. Geol.* **267**, 175–184.

Dideriksen K., Baker J. A. and Stipp S. L. S. (2008) Equilibrium Fe isotope fractionation between inorganic aqueous Fe(III) and the siderophore complex, Fe(III)–desferrioxamine B. *Earth Planet. Sci. Lett.* **269**, 280–290.

dos Santos Pinheiro G. M., Poitrasson F., Sondag F., Vieira L. C. and Pimentel M. M. (2013) Iron isotope composition of the suspended matter along depth and lateral profiles in the Amazon River and its tributaries. *J. S. Am. Earth Sci.* **44**, 35–44.

El Samrani A. G., Lartiges B. S., Ghanbaja J., Yvon J. and Kohler A. (2004) Trace element carriers in combined sewer during dry and wet weather: an electron microscope investigation. *Water Res.* **38**, 2063–2076.

Emmanuel S., Erel Y., Matthews A. and Teutsch N. (2005) A preliminary mixing model for Fe isotopes in soils. *Chem. Geol.* **222**, 23–34.

Escoube R., Rouxel O. J., Sholkovitz E. and Donard O. F. X. (2009) Iron isotope systematics in estuaries: the case of North River, Massachusetts (USA). *Geochim. Cosmochim. Acta* **73**, 4045–4059.

Fantle M. S. and DePaolo D. J. (2004) Iron isotopic fractionation during continental weathering. *Earth Planet. Sci. Lett.* **228**, 547–562.

Foster I. D. L. and Charlesworth S. M. (1996) Heavy metals in the hydrological cycle: trends and explanation. *Hydrol. Process.* **10**, 227–261.

Franke C., Kissel C., Robin E., Bonte P. and Lagroix F. (2009) Magnetic particle characterization in the Seine river system: implications for the determination of natural versus anthropogenic input. *Geochem. Geophys. Geosyst.* **10**.

Gaillardet J., Dupré B. and Allègre C. J. (1999) Geochemistry of large river suspended sediments: silicate weathering or recycling tracer? *Geochim. Cosmochim. Acta* **63**, 4037–4051.

Gaillardet J., Viers J. and Dupré B. (2005) Trace element in river waters. In *Treatise on Geochemistry 5. Surface and Ground Water Weathering and Soils*. Elsevier, pp. 225–272. ISBN 0-08-043751-6.

Guelke M. and von Blanckenburg F. (2007) Fractionation of stable iron isotopes in higher plants. *Environ. Sci. Technol.* **41**, 1896–1901.

Guelke M., von Blanckenburg F., Schoenberg R., Staubwasser M. and Stuetzel H. (2010) Determining the stable Fe isotope signature of plant-available iron in soils. *Chem. Geol.* **277**, 269–280.

Guilbaud R., Butler I. B. and Ellam R. M. (2011) Abiotic pyrite formation produces a large Fe isotope fractionation. *Science* **332**, 1548–1551.

Homoky W. B., Severmann S., Mills R. A., Statham P. J. and Fones G. R. (2009) Pore-fluid Fe isotopes reflect the extent of benthic Fe redox recycling: evidence from continental shelf and deep-sea sediments. *Geology* **37**, 751–754.

Houhou J., Lartiges B. S., Montarges-Pelletier E., Sieliechi J., Ghanbaja J. and Kohler A. (2009) Sources, nature, and fate of heavy metal-bearing particles in the sewer system. *Sci. Total Environ.* **407**, 6052–6062.

Icopini G. A., Anbar A. D., Ruebush S. S., Tien M. and Brantley S. L. (2004) Iron isotope fractionation during microbial reduction of iron: the importance of adsorption. *Geology* **32**, 205–208.

Ilina S. M., Poitrasson F., Lapitskiy S. A., Alekhin Y. V., Viers J. and Pokrovsky O. S. (2013) Extreme iron isotope fractionation between colloids and particles of boreal and temperate organic-rich waters. *Geochim. Cosmochim. Acta* **101**, 96–111.

Ingri J., Malinovsky D., Rodushkin I., Baxter D. C., Widerlund A., Andersson P., Gustafsson O., Forsling W. and Ohlander B. (2006) Iron isotope fractionation in river colloidal matter. *Earth Planet. Sci. Lett.* **245**, 792–798.

Johnson C. M. and Beard B. L. (2005) Biogeochemical cycling of iron isotopes. *Science* **309**, 1025–1027.

Lacan F., Radic A., Jeandel C., Poitrasson F., Sarthou G., Pradoux C. and Freydier R. (2008) Measurement of the isotopic composition of dissolved iron in the open ocean. *Geophys. Res. Lett.* **35**. http://dx.doi.org/10.1029/2008GL035841.

Lyven B., Hassellov M., Turner D. R., Haraldsson C. and Andersson K. (2003) Competition between iron- and carbon-based colloidal carriers for trace metals in a freshwater assessed using flow field-flow fractionation coupled to ICPMS. *Geochim. Cosmochim. Acta* **67**, 3791–3802.

Marechal C., Telouk P. and Albarede F. (1999) Precise analysis of copper and zinc isotopic compositions by plasma-source mass spectrometry. *Chem. Geol.* **156**, 251–273.

Martin J. H. (1990) Glacial-interglacial CO_2 change: the iron hypothesis. *Paleoceanography* **5**, 1–13.

Matthews A., Morgans-Bell H. S., Emmanuel S., Jenkyns H. C., Erel Y. and Halicz L. (2004) Controls on iron-isotope fractionation in organic-rich sediments (Kimmeridge Clay, Upper Jurassic, southern England). *Geochim. Cosmochim. Acta* **68**, 3107–3123.

Meybeck M., Lestel L., Bonte P., Moilleron R., Colin J. L., Rousselot O., Herve D., de Ponteves C., Grosbois C. and Thevenot D. R. (2007) Historical perspective of heavy metals contamination (Cd, Cr, Cu, Hg, Pb, Zn) in the Seine River basin (France) following a DPSIR approach (1950–2005). *Sci. Total Environ.* **375**, 204–231.

Morel F. M. M. and Price N. M. (2003) The biogeochemical cycles of trace metals in the oceans. *Science* **300**, 944–947.

Poitrasson F. (2006) On the iron isotope homogeneity level of the continental crust. *Chem. Geol.* **235**, 195–200.

Poitrasson F. and Freydier R. (2005) Heavy iron isotope composition of granites determined by high resolution MC-ICP-MS. *Chem. Geol.* **222**, 132–147.

Pokrovsky O. S. and Schott J. (2002) Iron colloids/organic matter associated transport of major and trace elements in small boreal rivers and their estuaries (NW Russia). *Chem. Geol.* **190**, 141–179.

Priadi C., Le Pape P., Morin G., Ayrault S., Maillot F., Juillot F., Hochreutener R., Llorens I., Testemale D., Proux O. and Brown, Jr., G. E. (2012) X-ray absorption fine structure evidence for amorphous zinc sulfide as a major zinc species in suspended matter from the seine river downstream of Paris, Ile-de-France, France. *Environ. Sci. Technol.* **46**, 3712–3720.

Radic A., Lacan F. and Murray J. W. (2011) Iron isotopes in the seawater of the equatorial Pacific Ocean: new constraints for the oceanic iron cycle. *Earth Planet. Sci. Lett.* **306**, 1–10.

Rocher V., Azimi S., Moilleron R. and Chebbo G. (2004) Hydrocarbons and heavy metals in the different sewer deposits in the 'Le Marais' catchment (Paris, France): stocks, distributions and origins. *Sci. Total Environ.* **323**, 107–122.

Rouxel O., Dobbek N., Ludden J. and Fouquet Y. (2003) Iron isotope fractionation during oceanic crust alteration. *Chem. Geol.* **202**, 155–182.

Rouxel O. J., Bekker A. and Edwards K. J. (2005) Iron isotope constraints on the Archean and Paleoproterozoic ocean redox state. *Science* **307**, 1088–1091.

Rouxel O., Shanks W. C., Bach, III, W. and Edwards K. J. (2008) Integrated Fe- and S-isotope study of seafloor hydrothermal vents at East Pacific rise 9–10 degrees N. *Chem. Geol.* **252**, 214–227.

Roy S., Gaillardet J. and Allegre C. J. (1999) Geochemistry of dissolved and suspended loads of the Seine River, France: anthropogenic impact, carbonate and silicate weathering. *Geochim. Cosmochim. Acta* **63**, 1277–1292.

Roy M., Rouxel O., Martin J. B. and Cable J. E. (2012) Iron isotope fractionation in a sulfide-bearing subterranean estuary and its potential influence on oceanic Fe isotope flux. *Chem. Geol.* **300**, 133–142.

Schoenberg R. and von Blanckenburg F. (2005) An assessment of the accuracy of stable Fe isotope ratio measurements on samples with organic and inorganic matrices by high-resolution multicollector ICP-MS. *Int. J. Mass Spectrom.* **242**, 257–275.

Severmann S., Johnson C. M., Beard B. L., German C. R., Edmonds H. N., Chiba H. and Green D. R. H. (2004) The effect of plume processes on the Fe isotope composition of hydrothermally derived Fe in the deep ocean as inferred from the Rainbow vent site, Mid-Atlantic Ridge, 36 degrees 14′ N. *Earth Planet. Sci. Lett.* **225**, 63–76.

Severmann S., Johnson C. M., Beard B. L. and McManus J. (2006) The effect of early diagenesis on the Fe isotope compositions of porewaters and authigenic minerals in continental margin sediments. *Geochim. Cosmochim. Acta* **70**, 2006–2022.

Severmann S., McManus J., Berelson W. M. and Hammond D. E. (2010) The continental shelf benthic iron flux and its isotope composition. *Geochim. Cosmochim. Acta* **74**, 3984–4004.

Sharma M., Polizzotto M. and Anbar A. D. (2001) Iron isotopes in hot springs along the Juan de Fuca Ridge. *Earth Planet. Sci. Lett.* **194**, 39–51.

Skulan J. L., Beard B. L. and Johnson C. M. (2002) Kinetic and equilibrium Fe isotope fractionation between aqueous Fe(III) and hematite. *Geochim. Cosmochim. Acta* **66**, 2995–3015.

Song L., Liu C.-Q., Wang Z.-L., Zhu X., Teng Y., Liang L., Tang S. and Li J. (2011) Iron isotope fractionation during biogeochemical cycle: information from suspended particulate matter (SPM) in Aha Lake and its tributaries, Guizhou, China. *Chem. Geol.* **280**, 170–179.

Staubwasser M., von Blanckenburg F. and Schoenberg R. (2006) Iron isotopes in the early marine diagenetic iron cycle. *Geology* **34**, 629–632.

Taylor S. R. and McLennan S. M. (1995) The geochemical evolution of the continental-crust. *Rev. Geophys.* **33**, 241–265.

Taylor P. D. P., Maeck R. and De Bievre P. (1992) Determination of the absolute isotopic composition and atomic weight of a reference sample of natural iron. *Int. J. Mass Spectrom.* **121**, 111–125.

Teutsch N., von Gunten U., Porcelli D., Cirpka O. A. and Halliday A. N. (2005) Adsorption as a cause for iron isotope fractionation in reduced groundwater. *Geochim. Cosmochim. Acta* **69**, 4175–4185.

Thévenot D., Meybeck M. and Lestel L. (2002) Métaux lourds: des bilans en mutation. *Rapport de synthèse PIREN-Seine 1998–2001*. p. 76. <http://www.sisyphe.upmc.fr/internet/piren/v2/modules/sections/>.

Thévenot D. R., Moilleron R., Lestel L., Gromaire M.-C., Rocher V., Cambier P., Bonte P., Colin J.-L., de Ponteves C. and Meybeck M. (2007) Critical budget of metal sources and pathways in the Seine River basin (1994–2003) for Cd, Cr, Cu, Hg, Ni, Pb and Zn. *Sci. Total Environ.* **375**, 180–203.

Thompson A., Ruiz J., Chadwick O. A., Titus M. and Chorover J. (2007) Rayleigh fractionation of iron isotopes during pedogenesis along a climate sequence of Hawaiian basalt. *Chem. Geol.* **238**, 72–83.

Wasylenki L. E., Anbar A. D., Liermann L. J., Mathur R., Gordon G. W. and Brantley S. L. (2007) Isotope fractionation during microbial metal uptake measured by MC-ICP-MS. *J. Anal. At. Spectrom.* **22**, 905–910.

Weyer S. and Schwieters J. B. (2003) High precision Fe isotope measurements with high mass resolution MC-ICPMS. *Int. J. Mass Spectrom.* **226**, 355–368.

Yesavage T., Fantle M. S., Vervoort J., Mathur R., Jin L., Liermann L. J. and Brantley S. (2012) Fe cycling in the Shale Hills Critical Zone Observatory, Pennsylvania: an analysis of biogeochemical weathering and Fe isotope fractionation. *Geochim. Cosmochim. Acta* **99**, 18–38.

Zwolsman J. J. G. and van Eck G. T. M. (1999) Geochemistry of major elements and trace metals in suspended matter of the Scheldt estuary, southwest Netherland. *Mar. Chem.* **66**, 91–111.

Associate editor: Nicolas Dauphas